Journal of Sound and Vibration (1997) **203**(5), 745–761

CONTROL OF AIRCRAFT INTERIOR NOISE USING GLOBALLY DETUNED VIBRATION ABSORBERS†

C. R. FULLER AND J. P. MAILLARD

Vibration and Acoustics Laboratories, Virginia Polytechnic Institute and State University, Blacksburg, VA. 24061-0238 U.S.A.

AND

M. MERCADAL AND A. H. VON FLOTOW

Hood Technology Corporation, Hood River, Oregon, 97031-9641 U.S.A.

(*Received* 8 *December* 1995, *and in final form* 2 *December* 1996)

A simplified analytical structural acoustics model of a propeller aircraft is developed to study the potential of mechanical vibration absorbers for reducing interior noise. The results show that globally detuning the absorbers to minimize an interior acoustic cost function gives attenuations of the order of 6–10 dB of the blade passage frequency interior noise when properly configured. The analysis also predicts that globally detuned absorbers consistently outperform tuned absorbers in which the base motion is directly minimized.

1. INTRODUCTION

The reduction of interior noise in aircraft still remains a challenge to aircraft designers and in recent years several advanced techniques have been considered. Tuned mechanical vibration absorbers designed to reduce the vibration of the aircraft fuselage, and hence its interior noise, have been developed and tested by a number of companies [1–3]. Sound reductions of the order of 8 to 10 dB in the fundamental blade passage frequency at cruise conditions with a weight penalty of about 25 kg have been reported. While this technique is fully passive and thus does not require any control energy, it suffers from a loss in performance when the absorbers are off-resonance, i.e., the propeller rotational speeds vary from the design point. A suggested solution to this problem would be to use absorbers whose properties could be adapted in order to track and remain tuned to the varying disturbance frequency.

Fully active solutions have also been considered. Recent flight tests have demonstrated the potential of an active control system termed Active Noise Control (ANC), which uses an array of acoustic control sources and error microphones distributed throughout the cabin space [4, 5]. Emerging commercial systems have been installed in aircraft such as the SAAB 340 or SAAB 2000 and typically comprise of 24–36 optimally located loudspeakers in conjunction with 48–72 error microphones. The total weight is around 70 kg for a 10 dB attenuation in the propeller fundamental frequency. Each speaker has a maximum power consumption of 25 Watts and approximately 1 km of wire is required in the SAAB 2000. The total power consumption of the system is approximately 300 Watts. The active noise control approach generally requires many control transducers. In addition, the performance tends to roll off at the higher harmonics of the propeller noise. An alternative,

†Paper originally presented at the 1st Joint CEAS/AIAA Aeroacoustics Conference, Munich, June, 1995.

0022–460X/97/250745 + 17 $25.00/0/sv960867

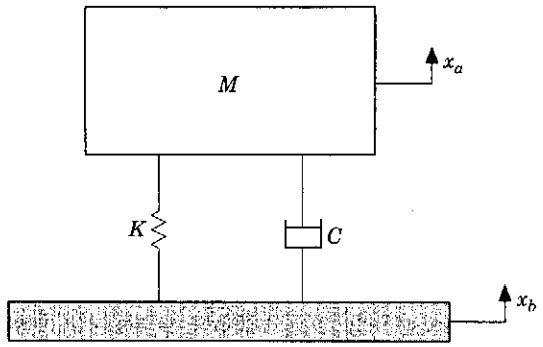

Figure 1. Mechanical vibration absorber schematic.

where M is the mass of the absorber, ω_r is the natural frequency of the absorber given by $\omega_r = \sqrt{K/M}$ and α is the ratio between the disturbance frequency and the natural frequency of the absorber, $\alpha = \omega/\omega_r$. The quality factor Q of the absorber is related to the damping and thus the sharpness of the absorber response peak at resonance and is defined as

$$Q = M\omega_r/C, \tag{2}$$

where C is the damping constant of the dash-pot. Note that with no damping ($C = 0$), the system's tuned impedance ($\alpha = 1$) becomes infinite and purely imaginary. In this case, the absorber will theoretically suppress the vibrations of anything it is attached to by exerting an infinitely large reactive force on the structure. Generally then, vibration absorbers with high MQ do not primarily "absorb" energy and the name is a misnomer. The expression of equation (1) can be approximated near resonance and for high-Q systems by

$$Z_a \approx M\mathrm{j}\alpha\omega_r/(1 - \alpha^2 + \mathrm{j}\alpha/Q). \tag{3}$$

It can be seen from equation (3) that the mechanical impedance of the absorber at resonance is $Z_a \approx M\omega_r Q$. Thus, operated at resonance, the dynamic impedance of the

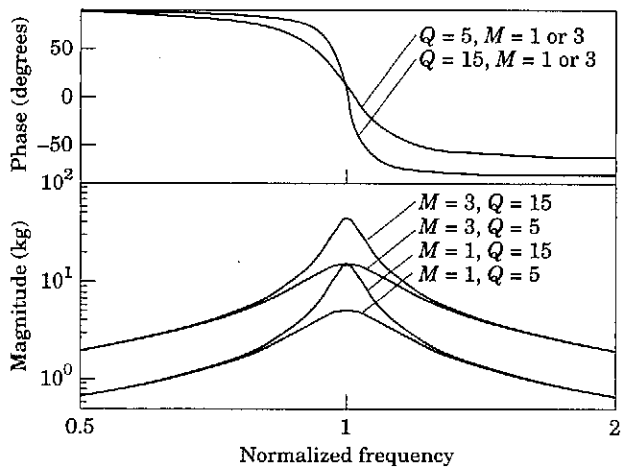

Figure 2. Normalized absorber impedance, Z_a/ω_r, as a function of M and Q.

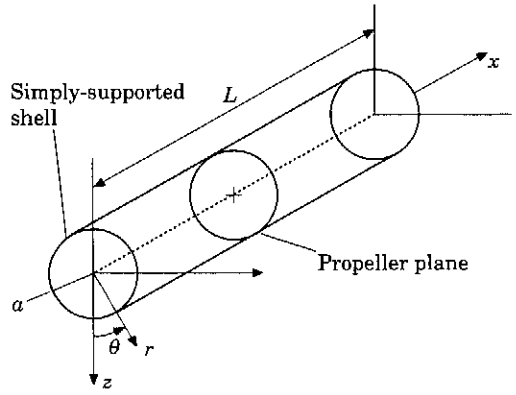

Figure 3. Co-ordinate system of the fuselage model.

2.2. FUSELAGE INTERIOR NOISE MODEL WITH VIBRATION ABSORBERS

In this analysis the aircraft fuselage dynamics and its acoustic behavior is modelled as a simply supported cylinder of length L, radius a, and thickness h as shown in Figure 3. The analysis is based upon a previous model developed by Silcox and Lester [8]. The cylinder is assumed to have rigid shear-diaphragm end caps. The input disturbance to the cylinder is represented by a harmonic, narrowband external pressure loading $p_d(x, \theta)\, e^{j\omega t}$ acting on the exterior of the cylinder. N vibration absorbers are mounted on the cylinder in order to alter the primary structural response due to the external pressure field. They can be modelled by a set of radially acting point forces, $F_i (i = 1, 2, \ldots, N)$. The amplitude F_i of the force exerted by the absorber on the structure is a function of the mechanical compliance of the ith absorber and the shell displacement at the mount location, (x_i, θ_i):

$$F_i = -Z_i^d \omega(x_i, \theta_i). \tag{6}$$

In the above equation Z_i^d relates the displacement of the ith absorber's base to the force acting back onto the base. It is defined as $Z_i^d = j\omega Z_a$, where Z_a is the mechanical impedance given in equation (1). The contribution of the N absorbers is expressed as a pressure input distribution of the form.

$$f^a(x, \theta) = \sum_{i=1}^{N} F_i \delta(x - x_i) \frac{\delta(\theta - \theta_i)}{a}, \tag{7}$$

where δ represents the Dirac delta function. The above distribution can be seen as the secondary "control" source while the external sound pressure field represents the primary "disturbance" source. Note that the secondary source is coupled to the cylinder displacement through the absorbers impedance $Z_i^d (i = 1, 2, \ldots, N)$.

Using standard thin shell theory [9] the normal displacement of the cylinder can be written as

$$\omega(x, \theta, t) = \left\{ \sum_{m=1}^{\infty} \sum_{n=0}^{\infty} W_{mn}^c \sin(\gamma_m x) \cos(n\theta) + \sum_{m=1}^{\infty} \sum_{n=1}^{\infty} W_{mn}^s \sin(\gamma_m x) \sin(n\theta) \right\} e^{j\omega t}, \tag{8}$$

where the complex coefficients, W_{mn}^c and W_{mn}^s, give the amplitude of the response of the cylinder in the (m, n)th vibration mode and $\gamma_m = m\pi/L$. Here m and n correspond to the modal order in the axial and circumferential direction, respectively.

longerons and frames by adding correction terms to the Donnell–Mushtari equations. The L_{33} entry given in equation (14) is modified as follows:

$$L_{33} = \Omega^2 - 1 - \beta^2(\mu_a \xi_m^4 + \mu_h n^4 + 2\mu_t \xi_m^2 n^2), \tag{15}$$

where the correction factors, μ_t, μ_a, and μ_h are given in Table 1. Including the density correction factor, μ_m, the longitudinal phase speed also becomes

$$c_L = \sqrt{E_d/\rho\mu_m(1 - \nu^2)}. \tag{16}$$

A matrix notation is now introduced to solve for the coupled response of the system with absorbers. The infinite summations in the previous equations are approximated by finite summations including the first N_{circ} circumferential modes and N_{long} longitudinal modes. Taking into account both sine and cosine circumferential modes, the total number of modes is $N_{\text{mode}} = 2N_{\text{circ}}N_{\text{long}}$. Let $\mathbf{q}$ represent the column vector of modal displacement amplitudes, W^c_{mn} and W^s_{mn}, $\mathbf{f}$ the column vector of absorber modal forces, F^c_{mn} and F^s_{mn}, and $\mathbf{f}^a$ the column vector of forces in the absorbers, F_i. Equation (6) can be written as

$$\mathbf{f}^a = -\mathbf{Z}\boldsymbol{\Phi}^a\mathbf{q}, \tag{17}$$

where $\mathbf{Z}$ is a $N \times N$ diagonal matrix containing the compliance terms $Z_i^d (i = 1, 2, \ldots, N)$, and $\boldsymbol{\Phi}^a$ is a $N \times N_{\text{mode}}$ matrix relating the modal amplitudes W^c_{mn} and W^s_{mn} to the radial displacements at the absorber locations, $w(x_i, \theta_i)$. Now the absorber forces, F_i, are expanded in terms of the cylinder mode shapes (equation (11)) to yield the absorber modal forces, F^c_{mn} and F^s_{mn}. This is written in matrix notation as

$$\mathbf{f} = \boldsymbol{\Psi}^a\mathbf{f}^a, \tag{18}$$

where $\boldsymbol{\Psi}^a$ is a $N_{\text{mode}} \times N$ matrix. Let $\mathbf{H}$ be the diagonal matrix containing the modal transfer functions $H_{mn}(\omega)$. Using equation (17) and equation (18), equation (12) is rewritten as

$$\mathbf{q} = \mathbf{Hp} - \mathbf{H}\boldsymbol{\Psi}^a\mathbf{Z}\boldsymbol{\Phi}^a\mathbf{q}, \tag{19}$$

where $\mathbf{p}$ is the column vector of external pressure modal components, $P^{d,c}_{mn}$ and $P^{d,s}_{mn}$. The displacement modal amplitudes of the coupled shell-absorber system are solutions of the linear system.

$$\mathbf{q} = \mathbf{A}^{-1}\mathbf{Hp}, \tag{20}$$

where

$$\mathbf{A} = \mathbf{I} + \mathbf{H}\boldsymbol{\Psi}^a\mathbf{Z}\boldsymbol{\Phi}^a. \tag{21}$$

It should be mentioned that the matrix $\mathbf{A}$ is not diagonal, i.e., the presence of the absorbers yields a coupling between the cylinder structural modes. With no absorbers, the cylinder

TABLE 1

Density and stiffness correction factors

Term	Expression
Density	$\mu_m = 1 + A_F/hS_F + A_L/hS_L$
Torsion	$\mu_t = hD_L^3/(h^3S_L/3)$
Axial bending	$\mu_a = 1 + (1/L_S S_L)(I_L + (D_L^2/4)[hS_L A_L/(hS_L + A_L)])$
Hoop bending	$\mu_h = 1 + (1/I_S S_F)(I_F + (D_F^2/4)[hS_F A_F/(hS_F + A_F)])$

where: A_F, A_L = frame and longeron cross-section area, D_F, D_L = frame and longeron height, S_F, S_L = frame and longeron spacing, I_F, I_L = frame and longeron area moment of inertia about neutral axis, respectively and I_S = skin area moment of inertia per unit length about neutral axis

where $\mathbf{q}^H$ represents the Hermitian transpose of $\mathbf{q}$. The second cost function is an estimate of the total acoustic potential energy inside the shell. It is defined as

$$J_{\text{acous}} = \frac{1}{4\rho c^2}\int_V |p(x, r, \theta)|^2 \, \mathrm{d}V \approx \frac{1}{4\rho c^2}\frac{2\pi L}{N_x N_\theta N_r}\sum_{i_x=1}^{N_x}\sum_{i_\theta=1}^{N_\theta}\sum_{i_r=1}^{N_r} r_i |p(r_i, x_i, \theta_i)|^2. \tag{26}$$

As seen in equation (1), the absorber impedance is a non-linear function of the detuning factor α_i which requires implementing a non-linear parametric optimization procedure. The search for a minimum is constrained by setting upper and lower bounds on the detuning factors. The optimization algorithm used in the calculations is based on Sequential Quadratic Programming (SQP) techniques, also referred to as constrained quasi-Newton methods. An overview of SQP is found in references [11] and [12]. The constrained quasi-Newton method assumes the cost function has a unique minimum. In cases where several minima can be found within the constraints, the optimized solution is not guaranteed to yield the global minimum of the cost function. For the current system, plotting both structural and acoustic cost functions versus the tuning factors, α_i, reveals several local minima. In other words, the following results do not necessarily present the very best possible detuning configuration. To reduce the computational load involved in the optimization, an analytical expression was derived for the gradient of both cost functions with respect to the detuning factors, thus avoiding the need for finite difference approximations.

3. RESULTS AND DISCUSSION

3.1. CHOICE OF CYLINDER FUSELAGE MODEL PARAMETERS

For the following simulations we choose to model the fuselage structure of a BAe 748 propeller aircraft that was previously modelled by Thomas *et al.* [13, 14]. As discussed in section 2.2. of this paper, the fuselage is modelled as a simply supported, homogeneous cylinder of finite length with rigid end caps which is identical to that used by Thomas *et al.* However, for the present model the additional effects of the hoop and axial bending stiffness introduced by the stringers and frames as outlined previously are also included.

Thus, in addition to the mass of the stringers and frames being accounted for by "smearing" of their mass distribution, their stiffness is also included. Consequently, while most of the cylinder properties given in Table 2 are identical to those used by Thomas *et al.*, the cylinder has a hoop and axial stiffness which is significantly different. A

TABLE 2

Parameters of the cylinder fuselage model

Parameter	Magnitude	Parameter	Magnitude
Cylinder length, L (m)	16	Frame:	
Cylinder radius, a (m)	1·3	Spacing S_F (m)	0·40
Cylinder thickness, h (m)	$1{\cdot}2 \times 10^{-3}$	Height, D_F (m)	0·09
Material density, ρ, (kg/m^3)	2700	Area, A_F (m^2)	$1{\cdot}8 \times 10^{-4}$
Young's modulus, E (N/m^2)	$7{\cdot}1 \times 10^{10}$	Area moment of inertia, I_F (m^4)	$8{\cdot}7 \times 10^{-7}$
Poisson's ratio; ν	0·31	Longeron:	
Speed of sound c (m/s)	343	Spacing, S_L (m)	0·40
Density of air, ρ (kg/m^2)	1·21	Height, D_L (m^2)	0·015
Structural damping, η_s	0·1	Area, A_L (m^2)	$0{\cdot}7 \times 10^{-4}$
Acoustic damping, η	0·1	Area moment of inertia, I_L (m^4)	$2{\cdot}7 \times 10^{-9}$

Two different types of cost function were considered as the basis for the optimization scheme for the adaptive absorbers considered in section 2.3. The first cost function as defined in equation (25) represents tht total kinetic energy associated with the shell's normal vibration. The second cost function given in equation (26) is an estimate of the total acoustic potential energy radiated inside the shell. It is constructed by summing the squared modulus of the interior pressure evaluated over a grid of equally distributed points inside the shell and weighted by each point's radius. This cost function's estimate is based on 500 points distributed throughout the cylinder interior ($N_x = 10$, $N_\theta = 10$, $N_r = 5$). Note that 2040 points were used to compute the potential acoustic energy before and after optimization ($N_x = 20$, $N_\theta = 17$, $N_r = 6$). Reduction of the acoustic cost function thus implies a global reduction of the interior sound levels. The upper and lower limits imposed on the detuning factors, α_i (see section 2.3.), were set to 0·56 and 5, respectively. With these values, the absorber optimized natural frequencies are constrained to stay between $0{\cdot}2\omega$ and $1{\cdot}8\omega$, where ω is the disturbance frequency.

3.4. FREQUENCY OF $f = 88$ HZ (BPF)

For the first results the disturbance frequency was set to $f = 88$ Hz, corresponding to the propeller blade passage frequency of the BAe 748 system. Figure 4 and later figures show the amplitudes of the shell response for the three cases of uncontrolled, tuned, and detuned represented in bar diagram form from left to right, respectively, for each mode (m, n). The shell response consists of both a cos $(n\theta)$ and sin $(n\theta)$ component as shown in equation (8). The values plotted in Figure 4 are obtained from the square root of the sum of the squares of the amplitudes and thus represent the amplitude of a cos $(n\theta)$ rotated to the position of maximum displacement. The results show that the shell response is dominated by $n = 1$ and 2 circumferential modal orders with a rotated origin at $\theta = -10{\cdot}66°$. The corresponding interior pressure decomposition of Figure 5 shows that the pressure is dominated also by the $n = 1$ and $n = 2$ modes but at differing relative strengths due to the value of the cylinder structural acoustic coupling. The interior pressure

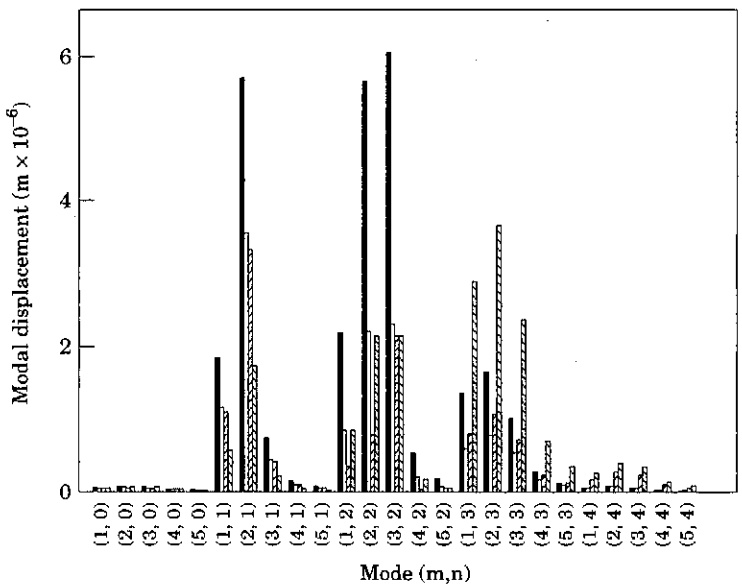

Figure 4. Structural response at 88 Hz: ■, uncontrolled; □, tuned; ▨, detuned, J_{struc}; ▧, detuned, J_{acous}.

0·95, 0·92, 0·95, and 5 for the respective absorber angular positions listed above. These values can be translated into a change of absorber stiffness using the relationship $K = M\omega^2$. Note that one of the above detuning factors has reached the upper limit set in the constrained optimization. Interestingly, a closer examination of this situation reveals that one of the optimally detuned absorbers is tending to zero stiffness (i.e., the absorbers are not present). Thus as well as optimizing the "active " component of the absorber, the approach of this paper also could be considered as simultaneously optimizing the "passive" component or mass distribution for example.

In the next case an interior acoustic potential energy is used as a cost function (a choice which seems the most logical since the objective is to globally reduce the interior sound levels). The shell and interior pressure modal amplitudes for this case are shown in Figures 4 and 5 along with the previous results. A similar trend is observed in the shell modal amplitudes as above. The $n = 1$ and $n = 2$ modes are reduced, however the $n = 3$ modal amplitudes are further increased over the results obtained with the cost function based on kinetic energy. The interior pressure modal amplitudes are all again reduced and to a further degree than when kinetic energy is used as a cost function. The reductions in the shell kinetic energy and the interior acoustic potential energy are 4·2 dB and 9·9 dB, respectively, when the acoustic potential energy is used as a cost function. The frequency detuning factors on the absorbers for this case are 0·74, 0·75, 1·06, and 0·62.

The results are summarized in Table 3. It is apparent that, at the BPF, globally detuning the absorbers leads to a significant improvement in reduction of the contained interior acoustic field over using individually tuned absorbers. This is an encouraging result especially for this "stiff" model where the shell modal density is lower at the BPF than previous fuselage studies of ASAC [13, 15]. Generally, better performance is achieved in ASAC when the modal density is higher.

3.5. FREQUENCY OF $f = 176$ HZ (2 BPF)

One now considers an identical set of simulation tests at twice the blade passing frequency or at the first harmonic of the propeller noise. Figures 6 and 7 show the modal amplitudes of the shell and interior pressure response at this higher frequency in the same format as previously. Also shown are the amplitudes with tuned absorbers and when globally detuned absorbers are used in conjunction with an interior acoustic potential energy cost function. The reductions in the acoustic potential energy for the test cases are summarized in Table 4. At this higher frequency the reduction in sound is not nearly as high as at $f = 88$ Hz. However, the globally detuned absorbers with both structural and acoustic based cost functions still perform better than tuned absorbers. Note that the two cost functions result in the same level of reductions. This suggests that vibration suppression rather than modal restructuring is the main mechanism of control at this frequency.

TABLE 3

Attenuation of shell kinetic energy and interior acoustic potential energy $f = 88$ Hz, $MQ = 750$ kg

	Δ Shell K.E. (dB)	Δ Acoustic P.E. (dB)
Tuned	6·4	4·3
Detuned (J_{struct})	8·4	5·0
Detuned (J_{acous})	4·2	9·9

TABLE 4

Attenuation of shell kinetic energy and interior acoustic potential energy $f = 176$ Hz, $MQ = 750$ kg

	Δ Shell K.E. (dB)	Δ Acoustic P.E. (dB)
Tuned	1·3	−0·2
Detuned (J_{struct})	3·6	2·2
Detuned (J_{acous})	3·6	2·2

is most likely due to the fact that, in the present configuration, the absorbers are poorly positioned so as to couple into the $n = 3$ mode. Two of the absorbers are located within 10° of an anti-node of the rotated $n = 3$ modal distribution and are thus unlikely to globally modify its vibration to any significant degree. In general, the number of absorbers needs to be at least twice the modal order of the motion to be controlled (Nyquist theory) and this would imply the use of six, appropriately positioned absorbers. Thus to control the higher BPF components, a system would most likely be composed of many absorbers with lighter masses. In this case, on the basis of the discussion in section 2.1., it would be necessary to keep the absorber Q as high as possible. The detuning factors in these cases were 0·78, 0·94, 1·23, and 0·91 for the structural cost function and 0·88, 1·24, 0·96, and 0·74 for the acoustic cost function.

3.6. ABSORBERS WITH A REDUCED MQ = 480, $f = 88$ HZ (BPF)

For the next test the mass of each individual absorber is reduced from 12·5 kg to 8 kg giving a system MQ of 480 kg. The attenuations in the acoustic field are then evaluated using tuned absorbers and globally detuned absorbers in conjunction with an acoustic potential energy cost function. The results are summarized in Table 5 and demonstrate that even for this absorber system with lighter masses, the globally detuned system still provides reasonable attenuations of the interior field (8·3 dB) and outperforms the tuned absorbers by over 4 dB. However, as expected from the discussion of section 2·1., the lighter absorber system gives reduced attenuation than the heavier system considered previously. The detuning factors in these cases were 0·56, 0·88, 1·05, and 0·63 for the structural cost function and 0·83, 0·85, 1·11, and 0.79 for the acoustic cost function.

3.7. FREQUENCY OF $f = 88$ HZ $\pm$ 5% (ROBUSTNESS STUDY)

In this last test, a brief study of the robustness of both the tuned and globally detuned absorber system to a change in disturbance or operating condition was conducted. Here the absorbers are optimized using an interior acoustic potential energy cost function at the cruise BPF. The characteristics of the absorbers are fixed, the frequency of the disturbance is then varied by +5% (to 92·4 Hz) and −5% (to 83·6 Hz) and the reductions

TABLE 5

Attenuation of shell kinetic energy and interior acoustic potential energy $f = 88$ Hz, $MQ = 480$ kg

	Δ Shell K.E. (dB)	Δ Acoustic P.E. (dB)
Tuned	6·3	4·2
Detuned (J_{struct})	6·3	7·0
Detuned (J_{acous})	4·5	8·3

3. H. J. HACKSTEIN, I. U. BORCHERS, K. RENGER and K. VOGT 1991 *In Proceedings of the DGLR/AIAA 14th Aeroacoustics Conference, Aachen, Germany, May* 11–14, *Paper No. DGLR/AIAA* 92-02-164. The Dornier 32 B Acoustic Test Cell (ATC) for interior noise tests and selected test results.
4. S. J. ELLIOTT, P. A. NELSON, I. M. STOTHERS and C. C. BOUCHER 1989 *Journal of Sound and Vibration* **128**, 355–357. Preliminary results of in-flight experiments on the active control of propeller-induced cabin noise.
5. C. M. DORLING, G. P. EATWELL, S. M. HUTCHINS, C. F. ROSS and S. G. C. SUTCLIFF 1989 *Journal of Sound and Vibration* **128**, 358–360. A demonstration of active noise reduction in an aircraft cabin.
6. C. R. FULLER and J. D. JONES 1987 *Journal of Sound and Vibration* **112**, 389–395. Experiments on reduction of propeller induced interior noise by active control of cylinder vibration.
7. M. A. SIMPSON, T. M. LUONG, C. R. FULLER and J. D. JONES 1989 *AIAA Paper* 89–1074. Full-scale demonstration tests on cabin noise reduction using active vibration control.
8. R. SILCOX and H. LESTER 1989 *AIAA Paper* 89–1123. Propeller modelling effects on interior noise in cylindrical cavities with application to active control.
9. A. W. LEISSA 1973 *Vibration of Shells*. NASA SP-288.
10. H. C. NELSON, B. ZAPOTOWSKI and M. BERNSTEIN 1958 *In National Specialists Meeting on Dynamics and Aeroelasticity*, Vibration analysis of orthogonally stiffened circular fuselage and comparison with experiment.
11. R. FLECHTER 1980 *Practical Methods of Optimization*. John Wiley; Volume 1 Constrained Optimization.
12. P. E. GILL, W. MURRAY and M. H. WRIGHT 1981 *Practical Optimization*. London: Academic Press.
13. D. R. THOMAS, P. A. NELSON and S. J. ELLIOTT 1994 *Journal of Sound and Vibration* **167**, 91–111. Active control of the transmission of sound through a thin cylindrical shell, part I: the minimization of vibrational energy.
14. D. R. THOMAS, P. A. NELSON and S. J. ELLIOTT 1994 *Journal of Sound and Vibration* **167**, 113–128. Active control of the transmission of sound through a thin cylindrical shell, part II: the minimization of the acoustic potential energy.
15. C. R. FULLER, C. H. HANSEN and S. D. SNYDER 1991 *Journal of Sound and Vibration* **145**, 195–215. Active control of sound radiation from a vibrating rectangular panel by sound sources and vibration inputs: an experimental comparison.